Altair® FluxMotor® 2026

Synchronous machines – Permanent magnets - Inner & Outer rotor

Motor Factory – Test – Characterization

General user information

Altairhyperworks.com

Contents

1 CHARACTERIZATION – OPEN CIRCUIT – MOTOR & GENERATOR – COGGING TORQUE

1.1 Overview

1.1.1 Positioning and objective

The aim of the test "**Characterization - Open circuit – Motor & Generator - Cogging torque**" is to get the characteristics of the cogging torque of the machine.
Thanks to this test it is possible to evaluate the impact of the machine topology (slots and magnets – number and dimensions) on the cogging torque characteristics (magnitude and period).

The following table helps to classify the test "Open circuit - Cogging torque".

Family	Characterization
Package	Open circuit
Convention	Motor & Generator
Test	Cogging Torque

Positioning of the test "Characterization - Open circuit – Motor & Generator - Cogging torque"

1.2 Main principles of computation

1.2.1 Cogging torque computation, overview

The electromagnetic torque computation is performed by using Magnetostatic application of Flux® (Finite Element software) inside FluxMotor®. The computation is done by considering multiple positions of the rotor.

To study electromagnetic devices, two types of energies (Magnetic field energy and co-energy) are considered.
The magnetic energy is expressed in terms of magnetic flux density B and magnetic field H by the following relation:

$$\mathrm{dWm} = \int_0^{\mathrm{B}} \vec{\mathrm{H}} \cdot \mathrm{d}\vec{\mathrm{B}}$$

The magnetic energy in a volume is given by the integral:

$$\mathrm{Wm} = \int_{\mathrm{V}} (\mathrm{dWm}) \times \mathrm{dV}$$

The magnetic co-energy is defined as:

$$\mathrm{dWm}' = \int_0^{\mathrm{H}} \vec{\mathrm{B}} \cdot \mathrm{d}\vec{\mathrm{H}}$$

The magnetic co-energy in a volume is given by the integral:

$$\mathrm{Wm}' = \int_{\mathrm{V}} (\mathrm{dWm}') \times \mathrm{dV}$$

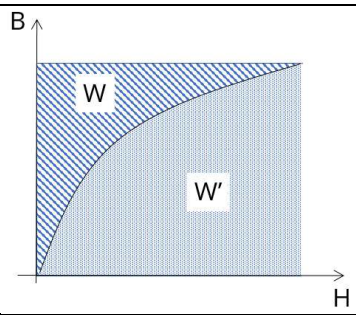

Illustration of magnetic energy and co-energy

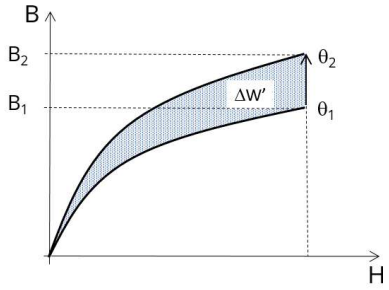

Variation of co-energy
during movement of rotation from θ_1 to θ_2

Depending on the position of the rotor (from θ_1 to $\theta_{2)}$, the reluctance of the system changes, causing a variation of magnetic flux density, represented by the colored area $\Delta W'$ on the right graph. This area represents the variation of the co-energy when moving from θ_1 to θ_2.

As there is no exciting current in the device during the cogging torque test, cogging torque will appear only due to permanent magnet.

The cogging torque is derived from the airgap flux and reluctance variation in the magnetic circuit with respect to rotor angular displacement.
The electromagnetic torque (T_{em}) can be derived by differentiating the magnetic field energy or total co-energy with respect to mechanical angle using virtual work method as:

$$T_{em} = -\frac{\partial W_m}{\partial \theta}$$

Where θ = rotor angular displacement.

Note: In case of relative important airgap length, the relative variation of airgap reluctance is low, and the resulting cogging torque magnitude can be very small.

1.2.2 Cogging torque period

The cogging torque period depends on the number of slots (N_S) and the number of poles (N_P).
It is given by the dividing 360°, circular mechanical degree in space, by the least common multiple of number of stator slots (N_S) and number of rotor poles (N_P).

$$\theta_{cog-perio} = \frac{360^{\circ}}{LCM(N_s, N_p)}$$

In general, with increasing number of slots and poles, cogging torque period decreases as shown in the following table.

POLES \ SLOTS	3	6	9	12	15	18	21	24	27	30	33	36	39	42	45	48	51	54	57	60	63	66	69	72	75	78	81	84	87	90
2	60,00	60,00	20,00	30,00	12,00	20,00	8,57	15,00	6,67	12,00	5,45	10,00	4,62	8,57	4,00	7,50	3,53	6,67	3,16	6,00	2,86	5,45	2,61	5,00	2,40	4,62	2,22	4,29	2,07	4,00
4	30,00	30,00	10,00	30,00	6,00	10,00	4,29	15,00	3,33	6,00	2,73	10,00	2,31	4,29	2,00	7,50	1,76	3,33	1,58	6,00	1,43	2,73	1,30	5,00	1,20	2,31	1,11	4,29	1,03	2,00
6			20,00			20,00			6,67			10,00			4,00			6,67			2,86			5,00			2,22			4,00
8		15,00	5,00	15,00	3,00	5,00	2,14	15,00	1,67	3,00	1,36	5,00	1,15	2,14	1,00	7,50	0,88	1,67	0,79	3,00	0,71	1,36	0,65	5,00	0,60	1,15	0,56	2,14	0,52	1,00
10			4,00	6,00	12,00	4,00	1,71	3,00	1,33	12,00	1,09	2,00	0,92	1,71	4,00	1,50	0,71	1,33	0,63	6,00	0,57	1,09	0,52	1,00	2,40	0,92	0,44	0,86	0,41	4,00
12			10,00			10,00			3,33			10,00			2,00			3,33			1,43			5,00			1,11			2,00
14				4,29	1,71	2,86	8,57	2,14	0,95	1,71	0,78	1,43	0,66	8,57	0,57	1,07	0,50	0,95	0,45	0,86	2,86	0,78	0,37	0,71	0,34	0,66	0,32	4,29	0,30	0,57
16				7,50	1,50	2,50	1,07	7,50	0,83	1,50	0,68	2,50	0,58	1,07	0,50	7,50	0,44	0,83	0,39	1,50	0,36	0,68	0,33	2,50	0,30	0,58	0,28	1,07	0,26	0,50
18									6,67									6,67									2,22			
20					6,00	2,00	0,86	3,00	0,67	6,00	0,55	2,00	0,46	0,86	2,00	1,50	0,35	0,67	0,32	6,00	0,29	0,55	0,26	1,00	1,20	0,46	0,22	0,86	0,21	2,00
22						1,82	0,78	1,36	0,61	1,09	5,45	0,91	0,42	0,78	0,36	0,68	0,32	0,61	0,29	0,55	0,26	5,45	0,24	0,45	0,22	0,42	0,20	0,39	0,19	0,36
24						5,00			1,67			5,00			1,00			1,67			0,71			5,00			0,56			1,00
26							0,66	1,15	0,51	0,92	0,42	0,77	4,62	0,66	0,31	0,58	0,27	0,51	0,24	0,46	0,22	0,42	0,20	0,38	0,18	4,62	0,17	0,33	0,16	0,31
28							4,29	2,14	0,48	0,86	0,39	1,43	0,33	4,29	0,29	1,07	0,25	0,48	0,23	0,86	1,43	0,39	0,19	0,71	0,17	0,33	0,16	4,29	0,15	0,29
30									1,33			2,00			4,00			1,33			0,57			1,00			0,44			4,00
32								3,75	0,42	0,75	0,34	1,25	0,29	0,54	0,25	3,75	0,22	0,42	0,20	0,75	0,18	0,34	0,16	1,25	0,15	0,29	0,14	0,54	0,13	0,25
34									0,39	0,71	0,32	0,59	0,27	0,50	0,24	0,44	3,53	0,39	0,19	0,35	0,17	0,32	0,15	0,29	0,14	0,27	0,13	0,25	0,12	0,24
36									3,33									3,33									1,11			
38										0,63	0,29	0,53	0,24	0,45	0,21	0,39	0,19	0,35	3,16	0,32	0,15	0,29	0,14	0,26	0,13	0,24	0,12	0,23	0,11	0,21
40										3,00	0,27	1,00	0,23	0,43	1,00	1,50	0,18	0,33	0,16	3,00	0,14	0,27	0,13	1,00	0,60	0,23	0,11	0,43	0,10	1,00
42											1,43				0,57			0,95			2,86			0,71			0,32			0,57
44											2,73	0,91	0,21	0,39	0,18	0,68	0,16	0,30	0,14	0,55	0,13	2,73	0,12	0,45	0,11	0,21	0,10	0,39	0,09	0,18
46												0,43	0,20	0,37	0,17	0,33	0,15	0,29	0,14	0,26	0,12	0,24	2,61	0,22	0,10	0,20	0,10	0,19	0,09	0,17
48												2,50			0,50			0,83			0,36			2,50			0,28			0,50
50													0,18	0,34	0,80	0,30	0,14	0,27	0,13	1,20	0,11	0,22	0,10	0,20	2,40	0,18	0,09	0,17	0,08	0,80
52													2,31	0,33	0,15	0,58	0,14	0,26	0,12	0,46	0,11	0,21	0,10	0,38	0,09	2,31	0,09	0,33	0,08	0,15
54																											2,22			
56														2,14	0,14	1,07	0,13	0,24	0,11	0,43	0,71	0,19	0,09	0,71	0,09	0,16	0,08	2,14	0,07	0,14
58															0,14	0,26	0,12	0,23	0,11	0,21	0,10	0,19	0,09	0,17	0,08	0,16	0,08	0,15	2,07	0,14
60															2,00			0,67			0,29			1,00			0,22			2,00
62																0,24	0,11	0,22	0,10	0,19	0,09	0,18	0,08	0,16	0,08	0,15	0,07	0,14	0,07	0,13
64																1,88	0,11	0,21	0,10	0,38	0,09	0,17	0,08	0,63	0,08	0,14	0,07	0,27	0,06	0,13
66																		0,61			0,26			0,45			0,20			0,36
68																	1,76	0,20	0,09	0,35	0,08	0,16	0,08	0,29	0,07	0,14	0,07	0,25	0,06	0,12
70																		0,19	0,09	0,86	0,57	0,16	0,07	0,14	0,34	0,13	0,06	0,86	0,06	0,57
72																		1,67									0,56			
74																			0,09	0,16	0,08	0,15	0,07	0,14	0,06	0,12	0,06	0,12	0,06	0,11
76																			1,58	0,32	0,08	0,14	0,07	0,26	0,06	0,12	0,06	0,23	0,05	0,11
78																					0,22			0,38			0,17			0,31
80																				1,50	0,07	0,14	0,07	0,50	0,30	0,12	0,06	0,21	0,05	0,50

Cogging torque period in mechanical degrees

Note: An extremely small cogging torque period implies the need of a very thin mesh to get accurate results (by using a low airgap mesh coefficient value – See advanced parameter definition). Thus, the number of elements in the corresponding model will be very high (it means a high mesh density).
In the case of a very small cogging torque period, consideration of the airgap length is also relatively important.

In these conditions it is not possible to get good results because the numerical error induced by the mesh (meshing noise) has the same magnitude order than the cogging torque.

Dedicated mesh methods are needed for such situations but are not yet implemented in FluxMotor®.
In those cases, the advanced solution is to export the model to Flux and to adapt the mesh manually to reach the expected accuracy.
For information, the following table gives a general idea of easy computations (green cells), difficult ones (orange cells) and in some instances impossible ones (red cells) in FluxMotor®.

POLES \ SLOTS	3	6	9	12	15	18	21	24	27	30	33	36	39	42	45	48	51	54	57	60	63	66	69	72	75	78	81	84	87	90
2	60,00	60,00	20,00	30,00	12,00	20,00	8,57	15,00	6,67	12,00	5,45	10,00	4,62	8,57	4,00	7,50	3,53	6,67	3,16	6,00	2,86	5,45	2,61	5,00	2,40	4,62	2,22	4,29	2,07	4,00
4	30,00	30,00	10,00	30,00	6,00	10,00	4,29	15,00	3,33	6,00	2,73	10,00	2,31	4,29	2,00	7,50	1,76	3,33	1,58	6,00	1,43	2,73	1,30	5,00	1,20	2,31	1,11	4,29	1,03	2,00
6			20,00			20,00			6,67			10,00			4,00			6,67			2,86			5,00			2,22			4,00
8		15,00	5,00	15,00	3,00	5,00	2,14	15,00	1,67	3,00	1,36	5,00	1,15	2,14	1,00	7,50	0,88	1,67	0,79	3,00	0,71	1,36	0,65	5,00	0,60	1,15	0,56	2,14	0,52	1,00
10			4,00	6,00	12,00	4,00	1,71	3,00	1,33	12,00	1,09	2,00	0,92	1,71	4,00	1,50	0,71	1,33	0,63	6,00	0,57	1,09	0,52	1,00	2,40	0,92	0,44	0,86	0,41	4,00
12			10,00			10,00			3,33			10,00			2,00			3,33			1,43			5,00			1,11			2,00
14				4,29	1,71	2,86	8,57	2,14	0,95	1,71	0,78	1,43	0,66	8,57	0,57	1,07	0,50	0,95	0,45	0,86	2,86	0,78	0,37	0,71	0,34	0,66	0,32	4,29	0,30	0,57
16				7,50	1,50	2,50	1,07	7,50	0,83	1,50	0,68	2,50	0,58	1,07	0,50	7,50	0,44	0,83	0,39	1,50	0,36	0,68	0,33	2,50	0,30	0,58	0,28	1,07	0,26	0,50
18									6,67									6,67									2,22			
20					6,00	2,00	0,86	3,00	0,67	6,00	0,55	2,00	0,46	0,86	2,00	1,50	0,35	0,67	0,32	6,00	0,29	0,55	0,26	1,00	1,20	0,46	0,22	0,86	0,21	2,00
22						1,82	0,78	1,36	0,61	1,09	5,45	0,91	0,42	0,78	0,36	0,68	0,32	0,61	0,29	0,55	0,26	5,45	0,24	0,45	0,22	0,42	0,20	0,39	0,19	0,36
24						5,00			1,67			5,00			1,00			1,67			0,71			5,00			0,56			1,00
26							0,66	1,15	0,51	0,92	0,42	0,77	4,62	0,66	0,31	0,58	0,27	0,51	0,24	0,46	0,22	0,42	0,20	0,38	0,18	4,62	0,17	0,33	0,16	0,31
28							4,29	2,14	0,48	0,86	0,39	1,43	0,33	4,29	0,29	1,07	0,25	0,48	0,23	0,86	1,43	0,39	0,19	0,71	0,17	0,33	0,16	4,29	0,15	0,29
30									1,33			2,00			4,00			1,33			0,57			1,00			0,44			4,00
32								3,75	0,42	0,75	0,34	1,25	0,29	0,54	0,25	3,75	0,22	0,42	0,20	0,75	0,18	0,34	0,16	1,25	0,15	0,29	0,14	0,54	0,13	0,25
34									0,39	0,71	0,32	0,59	0,27	0,50	0,24	0,44	3,53	0,39	0,19	0,35	0,17	0,32	0,15	0,29	0,14	0,27	0,13	0,25	0,12	0,24
36									3,33									3,33									1,11			
38										0,63	0,29	0,53	0,24	0,45	0,21	0,39	0,19	0,35	3,16	0,32	0,15	0,29	0,14	0,26	0,13	0,24	0,12	0,23	0,11	0,21
40										3,00	0,27	1,00	0,23	0,43	1,00	1,50	0,18	0,33	0,16	3,00	0,14	0,27	0,13	1,00	0,60	0,23	0,11	0,43	0,10	1,00
42												1,43			0,57			0,95			2,86			0,71			0,32			0,57
44											2,73	0,91	0,21	0,39	0,18	0,68	0,16	0,30	0,14	0,55	0,13	2,73	0,12	0,45	0,11	0,21	0,10	0,39	0,09	0,18
46												0,43	0,20	0,37	0,17	0,33	0,15	0,29	0,14	0,26	0,12	0,24	2,61	0,22	0,10	0,20	0,10	0,19	0,09	0,17
48												2,50			0,50			0,83			0,36			2,50			0,28			0,50
50													0,18	0,34	0,80	0,30	0,14	0,27	0,13	1,20	0,11	0,22	0,10	0,20	2,40	0,18	0,09	0,17	0,08	0,80
52													2,31	0,33	0,15	0,58	0,14	0,26	0,12	0,46	0,11	0,21	0,10	0,38	0,09	2,31	0,09	0,33	0,08	0,15
54																											2,22			
56														2,14	0,14	1,07	0,13	0,24	0,11	0,43	0,71	0,19	0,09	0,71	0,09	0,16	0,08	2,14	0,07	0,14
58															0,14	0,26	0,12	0,23	0,11	0,21	0,10	0,19	0,09	0,17	0,08	0,16	0,08	0,15	2,07	0,14
60															2,00			0,67			0,29			1,00			0,22			2,00
62																0,24	0,11	0,22	0,10	0,19	0,09	0,18	0,08	0,16	0,08	0,15	0,07	0,14	0,07	0,13
64																1,88	0,11	0,21	0,10	0,38	0,09	0,17	0,08	0,63	0,08	0,14	0,07	0,27	0,06	0,13
66																		0,61			0,26			0,45			0,20			0,36
68																	1,76	0,20	0,09	0,35	0,08	0,16	0,08	0,29	0,07	0,14	0,07	0,25	0,06	0,12
70																		0,19	0,09	0,86	0,57	0,16	0,07	0,14	0,34	0,13	0,06	0,86	0,06	0,57
72																		1,67									0,56			
74																			0,09	0,16	0,08	0,15	0,07	0,14	0,06	0,12	0,06	0,12	0,06	0,11
76																			1,58	0,32	0,08	0,14	0,07	0,26	0,06	0,12	0,06	0,23	0,05	0,11
78																					0,22			0,38			0,17			0,31
80																				1,50	0,07	0,14	0,07	0,50	0,30	0,12	0,06	0,21	0,05	0,50

Cogging torque computation: Green= easy / Orange = difficult / Red = very difficult or even impossible

To be noted that in case of square shape lamination, the analysis of the cogging torque will be done at least over 90 mechanical degrees (see the following example).

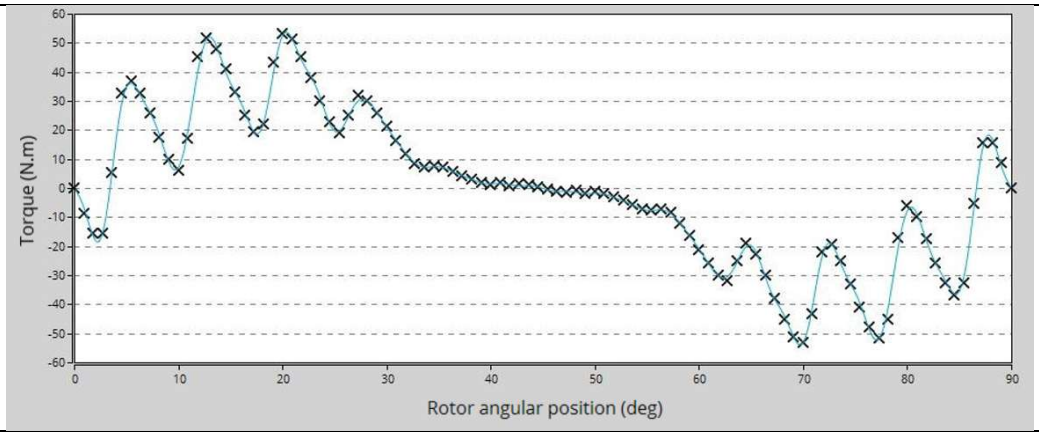

Cogging torque analysis over 90 mechanical degrees

2 CHARACTERIZATION – OPEN CIRCUIT – MOTOR & GENERATOR – BACK – EMF

2.1 Overview

2.1.1 Positioning and objective

The aim of the test "**Characterization - Open circuit – Motor & Generator - Back-EMF**" is to characterize the behavior of the machine when running in open circuit state.
The analysis of back-EMF characteristics is a first step to evaluate the relevance of the machine design regarding parameters such as: topology, winding architecture, composition of coils and choice of materials.

Warning! When a delta winding connection is considered, the computation doesn't consider circulation currents. That can lead to a different result than what expected in transient computation.
In such case it is recommended to perform a transient computation in Flux® environment. The application "Export to Flux" allows exporting this kind of model with the corresponding scenario ready to be solved.

The following table helps to classify the test "Open circuit – Back-EMF".

Family	Characterization
Package	Open circuit
Convention	Motor & Generator
Test	Back-EMF

Positioning of the test "Characterization - Open circuit – Motor & Generator - Back-EMF"

2.2 Main principles of computation

2.2.1 Back – emf computation

To get the Back-EMF versus time, the flux through each phase of the machine is computed for each rotor position over one half of electrical period.
Inside FluxMotor®, this computation is carried out using Magnetostatic application of Flux® (Finite Element software). The computation is done by considering multiple positions of the rotor.

A frequency analysis (Fast Fourier Transform F.F.T.) is then performed to extract the main harmonics of the signals.

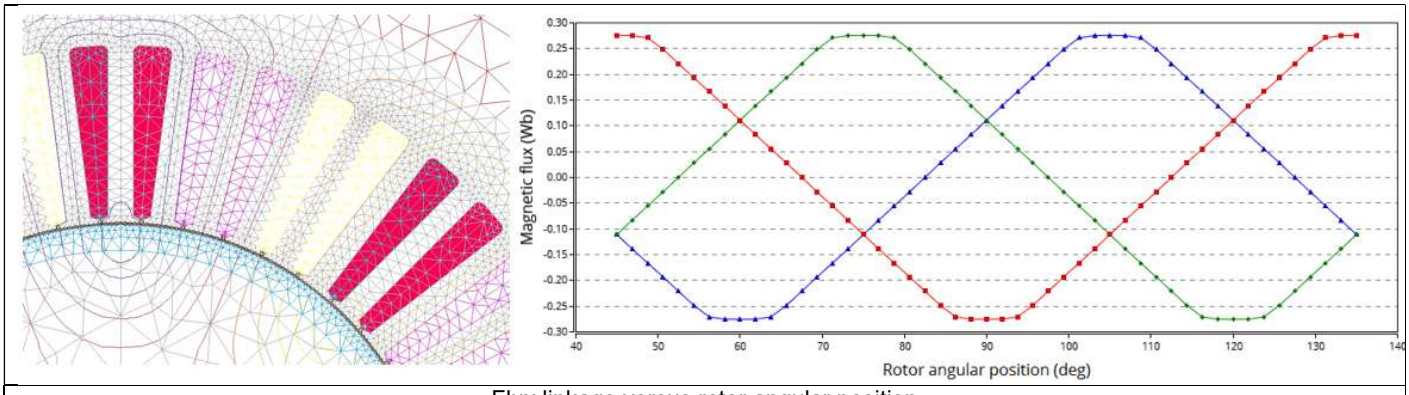

Flux linkage versus rotor angular position

The time variation of the phase voltage is deduced by derivation of the flux linkage. It is performed by considering the following formula:

$$E = \frac{d\Phi}{dt} = \frac{d\Phi}{d\theta} \times \frac{d\theta}{dt} = \frac{d\Phi}{d\theta} \times \Omega$$

Where Φ is the flux linkage and Ω is angular speed in rad/s.

The line-line voltages are deduced from the three phase voltages.

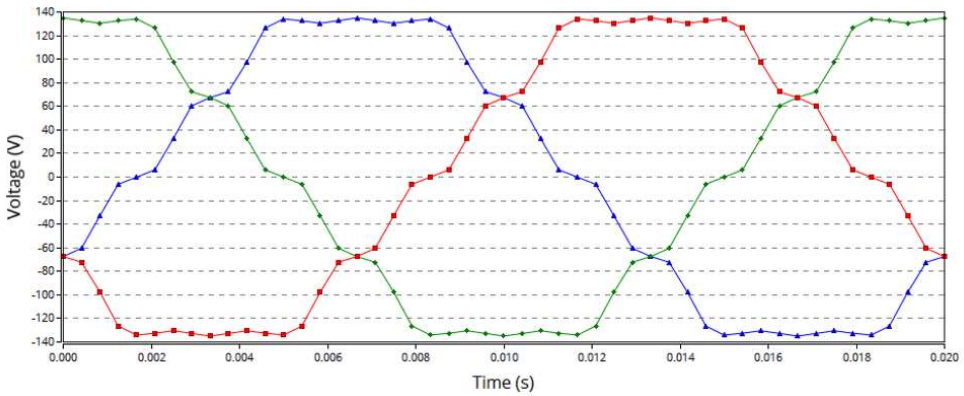

Open circuit - Line-Line voltage

2.2.2 Flux density in airgap

During the computation, a sensor put inside the airgap allows computing the flux density in the airgap versus rotor angular position.
It is located close to the stator bore diameter (at third quarter-length of airgap - stator side) in front of a stator tooth and remains motionless.

Like for the flux linkage, a Fast Fourier Transform is performed, and the main harmonics are extracted for flux density in airgap also.
The corresponding graphs and table are displayed.

3 CHARACTERIZATION – MODEL – MOTOR – MAPS

3.1 Positioning and objective

The aim of the test “Characterization - Model - Motor - Maps” is to give 2D maps in J_d-J_q plane for characterizing the 3-Phase synchronous machines with permanent magnets.

These maps allow predicting the behavior of the electrical rotating machine at a system level.

In this test engineers will find a system integrator and / or control-command tool adapted to their needs and able to provide accurate maps ready to be used in system simulation software like Activate or PSIM.

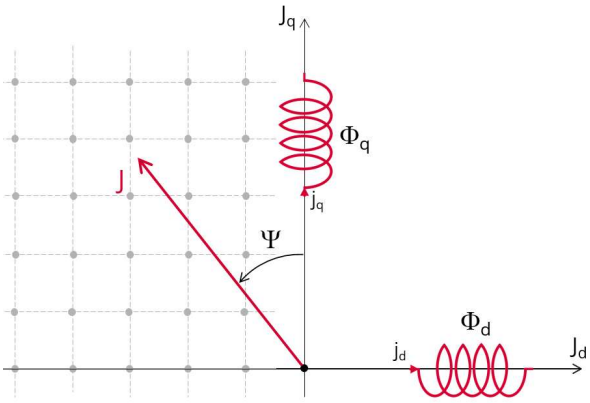

“Characterization - Model - Motor - Maps” illustration. Example for a second quadrant calculus.

Performance of the machine in steady state can be deduced from the results obtained in this test in association with the drive and control mode to be considered.

The following table helps to classify the test:

Family	Characterization
Package	Model
Convention	Motor
Test	Maps

Positioning of the test “Characterization - Model - Motor - Maps”

3.2 Main principles of computation

3.2.1 Flux linkage

One of the goals is to compute the D-axis and Q-axis flux linkage in the J_d, J_q plane.
To do that, a grid of values (J_d, J_q) is considered.
For each node of this grid, the corresponding flux linkage through each phase is extracted (Φ_a, Φ_b, Φ_c) through corresponding phases a, b, c). This is done using Finite Element modelling (Flux® software – Magnetostatic application).
D-axis flux-linkage component - Φ_d and **Q-axis flux-linkage component - Φ_q** are deduced according to Park's transformation.

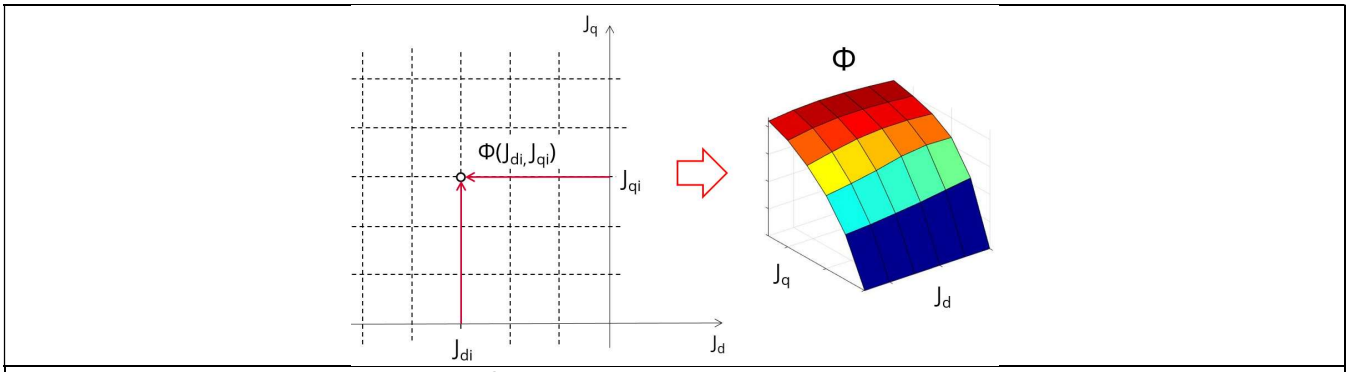

Computation on a grid in J_d, J_q plane

Our modeling considers cross-saturation. However, neither winding harmonics nor the variation of reluctance as a function of angular position of the rotor are considered.

Note: The impact on accuracy will be more important for machine with high level of saturation.
Iron loss computations are based on both a Finite Element modelling and on an analytical method where leakage flux between stator teeth is neglected.
In case of high level of saturation, this hypothesis leads to more errors particularly in the area where there is field weakening.

Note: In the examples shown in the images, positive value of J_d and positive value of J_q are considered. These values ranges correspond to the working conditions for a motor. However, the considered quadrants can be chosen through dedicated input (e.g., user can choose all quadrants, or only the 2nd, the 2nd and 3rd one, etc.) allowing the characterization of the machine behavior for other control conditions.

Note: In case the Rotor position dependency is set to "Yes", the computation is done in the J_d - J_q plane with an additional third axis corresponding to the rotor position θ_r.

3.2.2 Flux-linkage derivative respect to the rotor position

D-axis flux-linkage derivative with respect to the rotor position - $\Phi_d/d\theta_r$ and **Q-axis flux-linkage derivative with respect to the rotor position -** $\Phi_q/d\theta_r$ are computed from the flux linkage maps and using the following formulae:

$$\frac{\Delta\Phi_d}{\Delta\theta_r} \qquad \frac{\Delta\Phi_q}{\Delta\theta_r}$$

These maps are available only when the input Rotor position dependency is set to "Yes". The computation is done in the J_d - J_q plane with an additional third axis corresponding to the rotor position θ_r.

Note 1: The rotor position derivative is always in radians per second to simplify the usage of this map while considering the Park's voltage equations.

3.2.3 Dynamic inductances

D-axis synchronous inductance - $L_{d-dynamic}$ and **Q-axis synchronous inductance - $L_{q-dynamic}$** are computed from the flux linkage maps and using the following formulae:

$$L_{d-dynamic} = \frac{\Delta\Phi_d}{\Delta J_d} \qquad L_{q-dynamic} = \frac{\Delta\Phi_q}{\Delta J_q}$$

Note 1: The end-winding leakage inductance L_{endw}, computed in the winding area, is included in the computation of D-axis and Q-axis flux-linkage. The values of the dynamic inductances $L_{d-dynamic}$ and $L_{q-dynamic}$ consider the value of the end-winding inductance.

Note 2: In the previous formulae, one considers peak values for both flux and current.

Note 3: In case the Rotor position dependency is set to “Yes”, the computation is done in the J_d - J_q plane with an additional third axis corresponding to the rotor position θ_r.

3.2.4 Dynamic cross inductances

D-axis synchronous cross inductance - $L_{dq-dynamic}$ and **Q-axis synchronous cross inductance - $L_{qd-dynamic}$** are computed from the flux linkage maps and using the following formulae:

$$L_{dq-dynamic} = \frac{\Delta\Phi_d}{\Delta J_q} \qquad L_{qd-dynamic} = \frac{\Delta\Phi_q}{\Delta J_d}$$

Note 1: The end-winding leakage inductance Lendw, computed in the winding area, is included in the computation of D-axis and Q-axis flux-linkage. However, the values of the dynamic cross inductances Ldq–dynamic and Lqd-dynamic are not impacted by the end-winding inductance value since they are obtained with the derivative of respectively D-axis and Q-axis flux-linkage with respect to current variation along the corresponding quadrature axis (Q-axis and D-axis respectively).

Note 2: In the previous formulae, one considers peak values for both flux and current.

Note 3: In case the Rotor position dependency is set to “Yes”, the computation is done in the J_d - J_q plane with an additional third axis corresponding to the rotor position θ_r.

3.2.5 Static inductances

D-axis synchronous inductance - $L_{d-static}$ and **Q-axis synchronous inductance - $L_{q-static}$** are computed from the flux linkage maps and using the following formulae:

$$L_{d-static} = \frac{(\Phi_d - \Phi_0)}{\sqrt{2} \times J_d} \qquad L_{q-static} = \frac{\Phi_q}{\sqrt{2} \times J_q}$$

Note 1: The end-winding leakage inductance L_{endw}, computed in the winding area, is included in the computation of D-axis and Q-axis flux-linkage. The values of the static inductances $L_{d-static}$ and $L_{q-static}$ consider the value of the end-winding inductance.

Note 2: ϕ_0 corresponds to the permanent magnet flux included the cross-flux effects.

Note 3: In the previous formulae, one considers peak values for both flux and current.

Note 4: In case the Rotor position dependency is set to “Yes”, the computation is done in the J_d - J_q plane with an additional third axis corresponding to the rotor position θ_r.

3.2.6 Permanent magnet flux

The permanent magnet flux ϕ_0 corresponds to the magnetic flux provided by the magnet added to the magnetic flux provided by J_q along the q-axis.

As a result, ϕ_0 is a vector which corresponds to magnetic flux defined for $J_d = 0$, all along the q-axis.

Note: In case the Rotor position dependency is set to “Yes”, ϕ_0 is a vector that corresponds to magnetic flux defined for $J_d = 0$ and $\theta_r = 0$, all along the q-axis. To get values function of θ_r referred to the results given by the map **D-axis flux-linkage component - Φ_d**.

3.2.7 Electromagnetic torque

The **Electromagnetic torque** T_{em} is computed in different way in a function of the input Rotor position dependency value.

3.2.7.1 Rotor position dependency set to “No”

The flux linkage maps and the following formula are used:

$$T_{em} = \frac{m}{2} \times p \times \left(\Phi_d \times J_q - \Phi_q \times J_d\right)$$

Where m is the number of phases (3) and p is the number of pole pairs. J_d and J_q are the d and q axis peak current.

3.2.7.2 Rotor position dependency set to “Yes”

The **Electromagnetic torque T_{em}** is computed thanks to finite element computation and virtual work method to get the best evaluation of the ripple torque.

Note: In case the Rotor position dependency is set to “Yes”, **Electromagnetic torque T_{em}** average value computed with the Park’s equation or with virtual works are equal.

3.2.8 Iron loss computation

The **iron losses** are computed in a different way in the function of the value of the “Rotor position dependency” input.

3.2.8.1 Rotor position dependency set to “No”

A dedicated process has been developed to compute the **stator iron losses** (rotor iron losses not computed).
Stator iron losses are computed only for the stator magnetic circuit built with lamination material (computation is not applicable for solid materials).

Our method of computation doesn’t allow computing iron losses on the rotor side. However, iron loss level is generally not very important on the rotor side in comparison with iron losses on the stator side.

For each node of the grid, in the J_d-J_q space defined and illustrated above, magnetic flux densities in stator teeth are obtained from a dedicated semi-numerical method based on the integration of the flux density in the airgap.

For each considered region (foot teeth, teeth and yoke) we get the magnetic flux density as a function of the angular position. Then, the derivative of each magnetic flux density is computed as a function of the angular position.

At last, for each considered speed, a mathematical transformation is applied to get the derivative of magnetic flux density as a function of time

$$\frac{dB}{dt}(t) = \frac{dB}{d\theta}(\theta) \times \frac{d\theta}{dt}$$

Total iron losses are computed considering the magnetic circuit volume, the density of materials used, and the stacking coefficient considered for the stator lamination.

3.2.8.2 Rotor position dependency set to “Yes”

The **iron losses, stator and rotor** are computed thanks to the magnetostatic application of Flux (Finite Element modeling - MS FE) based on the magnetic flux derivative obtained over the finite element meshing.

The accuracy obtained is the same as the one with a magnetic transient finite element computation (MT FE) and for a given scenario the MS FE computation time is approximately reduced by a factor 2 times lower than MT FE.

3.2.8.3 Model used to compute iron losses

The model used to compute iron losses (W_{iron}) is:

$$W_{iron} = \left[\left(K_h \cdot \left(\frac{B_{max}}{K_f} \right)^{\alpha_h} \cdot f^{\beta h} \right) + \left(K_c \cdot \frac{1}{T_{elec}} \cdot \int_0^{Telec} \left[\frac{\left(\frac{dB}{dt} \right)}{K_f} \right]^{\alpha_c} dt \right) + \left(K_e \cdot \frac{1}{T_{elec}} \int_0^{Telec} \left[\frac{\left(\frac{dB}{dt} \right)}{K_f} \right]^{\alpha_e} dt \right) \right] . V_{iron} . K_f$$

With:
B_{max}: Peak value of the magnetic flux density (T)
f: Electrical frequency (Hz)
V_{iron}: Stator core lamination volume
K_f: Stacking factor

The other parameters of this model are defined in the application dedicated to materials in FluxMotor®, i.e. “Materials”.

Note: In case the “Rotor position dependency” input is set to “No”, the impact on accuracy will be more important for machine with high level of saturation. In fact, the semi-numerical method used to compute magnetic flux density of the stator teeth neglects flux leakage between teeth. This hypothesis will lead to more errors particularly in areas where there is field weakening (generally applicable at high speeds).

3.2.9 Joule losses

Joule losses in stator winding W_{Cus} are computed using the following formulae:

$$W_{Cus} = m \times R_{ph} \times (J)^2$$

$$\underline{J} = J_d + jJ_q$$

$$\left| \underline{J} \right| = J = \sqrt{J_d^2 + J_q^2}$$

Where m is the number of phases (3 in the first version of FluxMotor®),
J is the rms value of the phase current (I is the line current. I = J with a Wye winding connection),

R_{ph} is the phase resistance computed according to the temperatures defined by user in the test settings.

Note 1: R_{ph} considers the resistance factor defined in the winding settings (DESIGN area of Motor Factory).

Note 2: In case the Rotor position dependency is set to “Yes”, the computation is done in the J_d - J_q plane with an additional third axis corresponding to the rotor position θ_r.

3.2.10 Mechanical losses

The mechanical losses are computed as a function of the speed.
For more details, please refer to the document: MotorFactory_SMPM_IOR_3PH_Test_Introduction – section “Mechanical loss model settings”

3.2.11 Total losses

For each considered value of speed and currents J_d, J_q, the amount of losses described above (iron loss, Joule loss and mechanical losses) is computed and displayed.

Note: In case the Rotor position dependency is set to “Yes”, the computation is done in the J_d - J_q plane with an additional third axis corresponding to the rotor position θ_r.

4 CHARACTERIZATION – DATASHEET – MOTOR – I, U

4.1 Overview

4.1.1 Positioning and objective

The aim of the test "**Characterization - Datasheet – Motor – I, U**" is to characterize the behavior of the machine when operating at the working point that is located at the base speed point.
The working point or base speed point of the torque-speed curve is defined by considering the maximum allowed line-line voltage and the maximum allowed line current.

Note: In FluxMotor® terminology, the last working point on the constant torque part of the torque-speed curve is called "Base speed point" only when it is obtained for the maximum allowed line-line voltage and the maximum line current. If it is not the case, we called as "Corner speed point".

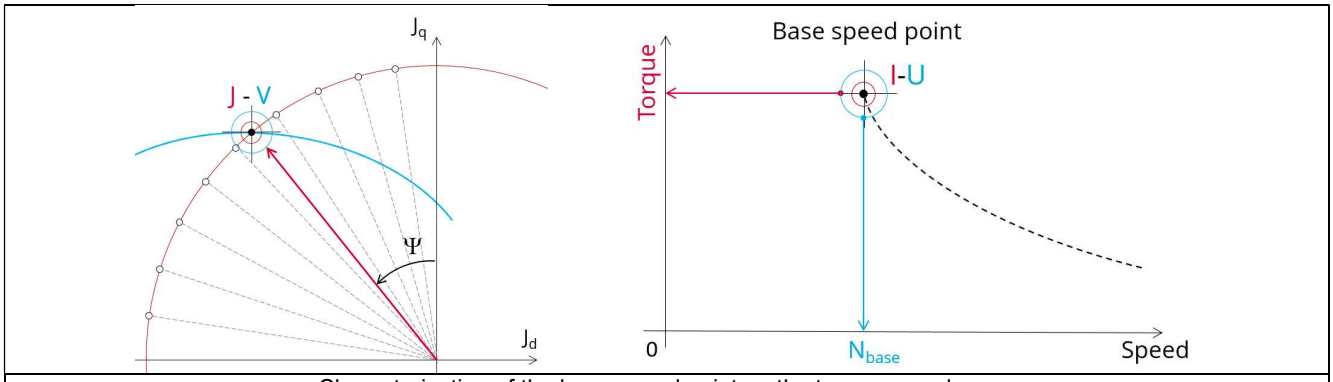

Characterization of the base speed point on the torque speed curve

This test gives an overview of the electromagnetic analysis of the motor considering the machine topology, the maximum allowed supplied line-line voltage and line current.
For this working point, general data of the machine, like machine constants, power balance and magnet behavior are computed and displayed. The magnetic flux density is also computed in every part of the machine to evaluate the design.

The test results also include all the necessary constants to build the equivalent model of the machine and to simulate the behavior of the machine in its electrical environment. In the results, a set of inductances is computed (unsaturated and at the base speed point).
The ripple torque at the base speed point is computed.
An overview of the machine performance at no-load is also given in this test.

The following table helps to classify the test "Characterization – Datasheet – Motor – I, U".

Family	Characterization
Package	Datasheet
Convention	Motor
Test	I, U

Positioning of the test "Characterization – Datasheet – Motor – I, U"

4.2 Main principles of computation

4.2.1 Introduction

The aim of this test is to give a good overview of the electromagnetic potential of the machine by characterizing the base speed point of the torque speed curve.

For this, several computation processes are involved:

- Determination of base speed point,
- Analysis of the electromagnetic behavior
- Computation of the ripple torque
- Computation of unsaturated inductances
- Computation of inductances at the base speed point
- Computation of open circuit characteristics

4.2.2 Determination of the base speed point

The base speed point of the torque speed curve corresponds to the working point obtain by considering the maximum allowed values of line current and line-line voltage ($I_{max.}$ and $U_{max.}$).

The quarter of circle corresponding to the maximum phase current in the J_d-J_q plane is discretized by considering the number of computations for control angle (Ψ) which is a user input parameter.

Several quantities, like the flux in the coils and flux density in (teeth and yoke of the machine) regions are computed as a function of the control angle (Ψ).
These computations are done by using Finite Element Modelling (Flux® software – Magnetostatic application).

- $\Phi d = f(\Psi)$
- $\Phi q = f(\Psi)$
- $B = f(\Psi)$

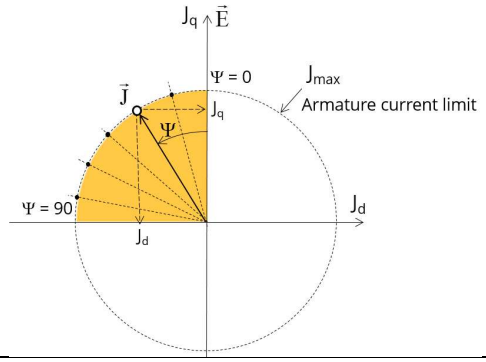

Discretization of the circle corresponding to $J_{max.}$

Then, an optimization process is performed to get the base speed point which corresponds to the working point at maximum line current and maximum line-line voltage: $I = I_{max.}$ and $U = U_{max.}$.

The resulting data (called general data) include:

- The control angle (Ψ) and thereby J_d and J_q
- The base speed
- The electrical frequency
- The torque
- The voltage components (V_d, V_q)

In addition, the power balance and machine constants are computed for the base speed point.
The torque constant “kT” is computed.

4.2.3 Electrical synchronous machines – Parameters and equations

For more details, please refer to the document: MotorFactory_SMPM_IOR_3PH_Test_Introduction – section “Electrical machine – Theoretical equations”.

4.2.4 Electromagnetic behavior

4.2.4.1 Flux in airgap

Thanks to a static computation (1 rotor position to be considered) done with results obtain for the base speed point (with line current, control angle and speed obtained for the base speed point), the airgap flux density is computed along a path in the airgap in Flux® software.
The resulting signal is obtained over at least one electric period (rebuilt if less than an electrical period represented in Flux® software). The average and the peak value of the flux density are computed. A harmonic analysis of the flux density in airgap versus rotor position is done to compute the magnitude of the first harmonic of the flux density.

These quantities are also computed for the “Flux per pole”.

4.2.4.2 Flux density in iron

Mean and maximum values of flux density of each iron region are computed thanks to sensors in Flux® software.

4.2.4.3 Magnet behavior

Mean values of flux density and magnetic field inside the magnets are computed over one ripple torque period thanks to sensors in Flux® software. Based on these results, demagnetization rate of the magnets is computed.

4.2.5 Ripple torque

A specific computation is performed to determine precisely the rate of ripple torque.
Considering J_d and J_q at the base speed point, a computation is performed over one ripple torque period by using Finite Element modelling (Flux® software – Magnetostatic application).
Many computation points are considered over the ripple torque period (advanced user input: **No. comp. / ripple period**).
The following steps are performed to determinate the mechanical torque.

4.2.5.1 Original computation of the electromagnetic torque

The magnetic torque exerted on a non-deformable part of the study domain is computed by the virtual work method. The torque in a given direction is obtained by deriving the system energy with respect to a virtual displacement of the part in this direction.
The magnetic torque T_{em} is given by the following derivative:

$$T_{em} = -\frac{\partial W_m}{\partial \theta}$$

$\partial\theta$ = elementary angular displacement,
W_m = magnetic energy in a volume region

The electromagnetic ripple torque is computed over the ripple torque period versus the rotor angular position $T_{em,\theta}$. The mean value “$T_{em,\ mean}$” is computed

4.2.5.2 Mechanical ripple torque based on Park’s model

The mechanical ripple torque must be computed at the base speed.
First, we compute the electromagnetic torque “$T_{em,\ Park}$” with Park’s model:

$$T_{em,Park} = \frac{m}{2} \times p \times \left(\Phi_d \times J_q - \Phi_q \times J_d\right)$$

Then, the iron loss torque, the mechanical loss torque and the additional loss torque are subtracted from “$T_{em,\ Park}$ “ to get the corresponding mean value of the mechanical torque “$T_{mech,\ Park}$”.

4.2.5.3 Resulting mechanical torque versus rotor angular position

To compute the resulting mechanical ripple torque, the original electromagnetic torque previously computed is weighted by the ratio of the mean value of the mechanical torque based on Park's model ($T_{mech, Park}$) and of the mean value of the original electromagnetic ripple torque ($T_{em, mean}$).

$$T_{mech.,\theta} = T_{em,\theta} \times \frac{T_{mech,Park}}{T_{em,mean}}$$

The peak-peak value of the mechanical ripple torque is then computed. The rate of ripple torque is deduced as a percentage or per unit of the nominal torque.

Warning: When the ripple torque computation is not requested, the computation of the working point is performed by considering only one position within the electrical period. It means that all the data characterizing the behavior of the machine can change based on the selection of ripple torque (Yes/No).
Flux density in magnetic circuit and the magnet behavior will be more accurately computed when the computation of the ripple torque will be requested.

4.2.6 Inductances

4.2.6.1 Unsaturated inductances

1) Initial conditions

To compute the unsaturated inductances, the reference phase (Phase 1) is supplied with a very low DC current.

The value of this DC current J_{dc} is computed as follows:

$$J_{dc} = k_J \times (J_{rms})_{max}$$

k_J is the current constant defined as an advanced user input parameter (default value = 0.05)
$(J_{rms})_{max}$ is the maximum phase current (rms value) deduced from the standard user input parameter "**Max. Line current**" by considering the winding connection (Y or Δ).

Note: To perform this computation, the magnets are replaced by a solid material with the same relative magnetic permeability.

2) Test description

The computation is performed by using Finite Element modelling (Flux® software – Magnetostatic - application).
The reference phase (Phase 1) is supplied with a DC current and the rotor rotates over a range of angular positions corresponding to one electrical period (= 2 poles).

The flux linkages through all the phases are computed over this equivalent electrical period.
Considering a linear behavior of the magnetic circuit, fluxes Φ_1, Φ_2, Φ_3, through phases 1, 2 and 3 respectively are defined as follows:

$$\begin{pmatrix} \Phi_1 \\ \Phi_2 \\ \Phi_3 \end{pmatrix} = \begin{vmatrix} L_1 & L_{12} & L_{13} \\ L_{21} & L_2 & L_{23} \\ L_{31} & L_{32} & L_3 \end{vmatrix} \times \begin{pmatrix} J_1 \\ J_2 \\ J_3 \end{pmatrix}$$

L_i is the self-inductances of phase "i",
L_{ij} is the mutual inductances between phases "i" and "j"

Self-inductance and mutual inductances are computed as a function of rotor angular position θ.
Considering the initial conditions of our computation, expression for self-inductance for the phase 1 is:

$$L_1 = L_{1av} + L_{2h} \times \mathrm{Cos}(2\theta)$$

$L_{i\,av}$ is the average value of the self-inductance L_i
L_{2h} is the first harmonic of the frequency representation of L_i

Considering the initial conditions of our computation, expression for mutual inductances between phases 1, 2 and 3 are:

$$L_{12} = L_{12av} + L_{2h} \times \mathrm{Cos}\left(\theta - \frac{\pi}{3}\right)$$
$$L_{13} = L_{12av} + L_{2h} \times \mathrm{Cos}\left(\theta + \frac{\pi}{3}\right)$$

$L_{ij\ av}$ is the average value of the mutual inductance L_{ij}
L_{2h} is the first harmonic of the frequency representation of L_{ij}

Using Park's equations and the corresponding transformation the D-axis and Q-axis flux linkages can be deduced:

$$\begin{pmatrix}\Phi_d\\ \Phi_q\\ \Phi_0\end{pmatrix} = \begin{vmatrix}\mathrm{Cos}\ (\theta) & \mathrm{Cos}\left(\theta - \frac{2\pi}{3}\right) & \mathrm{Cos}\left(\theta + \frac{2\pi}{3}\right)\\ \mathrm{Sin}\ (\theta) & \mathrm{Sin}\left(\theta - \frac{2\pi}{3}\right) & \mathrm{Sin}\left(\theta + \frac{2\pi}{3}\right)\\ \frac{1}{2} & \frac{1}{2} & \frac{1}{2}\end{vmatrix} \times \begin{pmatrix}\Phi_1\\ \Phi_2\\ \Phi_3\end{pmatrix}$$

The D-axis and Q-axis unsaturated inductances can be deduced as:

$$L_d = L_{1av} - L_{12av} + \frac{3}{2} \times L_{2h}$$
$$L_q = L_{1av} - L_{12av} - \frac{3}{2} \times L_{2h}$$

Note: The end-winding leakage inductance L_{endw} is considered as a part of L_{1av}.

The slot leakage inductance (L_{lk_slot}) is computed from the magnetic energy stored in the slots along the half part of the airgap close to the stator bore diameter.
The total value of the leakage inductance (L_{lk}) is computed as follows:

$$L_{lk} = L_{endw} + L_{lk\_slot}$$

The D-axis and Q-axis magnetization inductances are deduced using the following formulae:

$$L_{md} = L_d - L_{lk}$$
$$L_{mq} = L_q - L_{lk}$$

4.2.6.2 Inductances at the base speed point

Considering the base point defined by (J_d, J_q), low variations of current (corresponding to ΔJ_d, ΔJ_q) are injected into the stator phases. The resulting variation of D-axis and Q-axis flux linkage are computed.
D-axis synchronous inductance - L_d and **Q-axis synchronous inductance - L_q** are obtained by using the following formulae:

$$L_d = \frac{\Delta\Phi_d}{\Delta J_d} \qquad L_q = \frac{\Delta\Phi_q}{\Delta J_q}$$

Note 1: The end-winding leakage inductance L_{endw}, computed in the winding area, is included in the computation of D-axis and Q-Axis flux linkage. The values of the synchronous inductances L_d and L_q consider the value of the end-winding inductance.

Note 2: In the previous formulae, one considers peak values for both flux and current.

4.2.7 Open circuit

The same principles as for the "**Characterization - Open circuit – Motor & Generator - Back-EMF**" test is used. For information, see the corresponding section.

5 CHARACTERIZATION – THERMAL – MOTOR & GENERATOR – STEADY STATE

5.1 Overview

5.1.1 Positioning and objective

The aim of “Characterization – Thermal – Motor & Generator – Steady state” test is to evaluate the impact of electromagnetic performance on thermal behavior of the machine.
A thermal working point defined by a speed and a set of losses can be considered to compute the temperature charts and the main thermal parameters. The inputs describing the thermal working point can be set manually or imported from electromagnetic tests that were previously solved.

This test helps to answer the following questions:

- Can the machine operate at the targeted working point without any overheating? Yes / No
- Can the different kinds of proposed cooling help to reach good performance? Yes / No

The following table helps to classify the test “Characterization – Thermal – Motor & Generator – Steady state”.

Family	Characterization
Package	Thermal
Convention	Motor & Generator
Test	Steady state

Positioning of the test “Characterization – Thermal – Motor & Generator – Steady state”.

5.2 Main principles of computation

5.2.1 Introduction

Here are illustrations which give an overview of the thermal test:

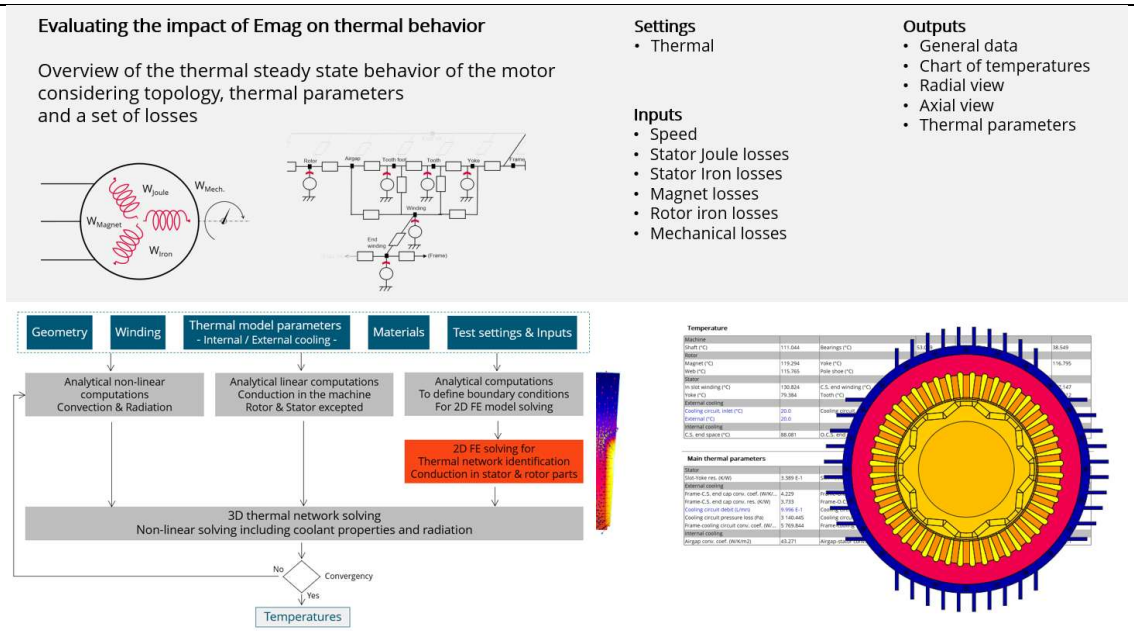

Characterization – Thermal – Steady state – Synchronous machine - Overview

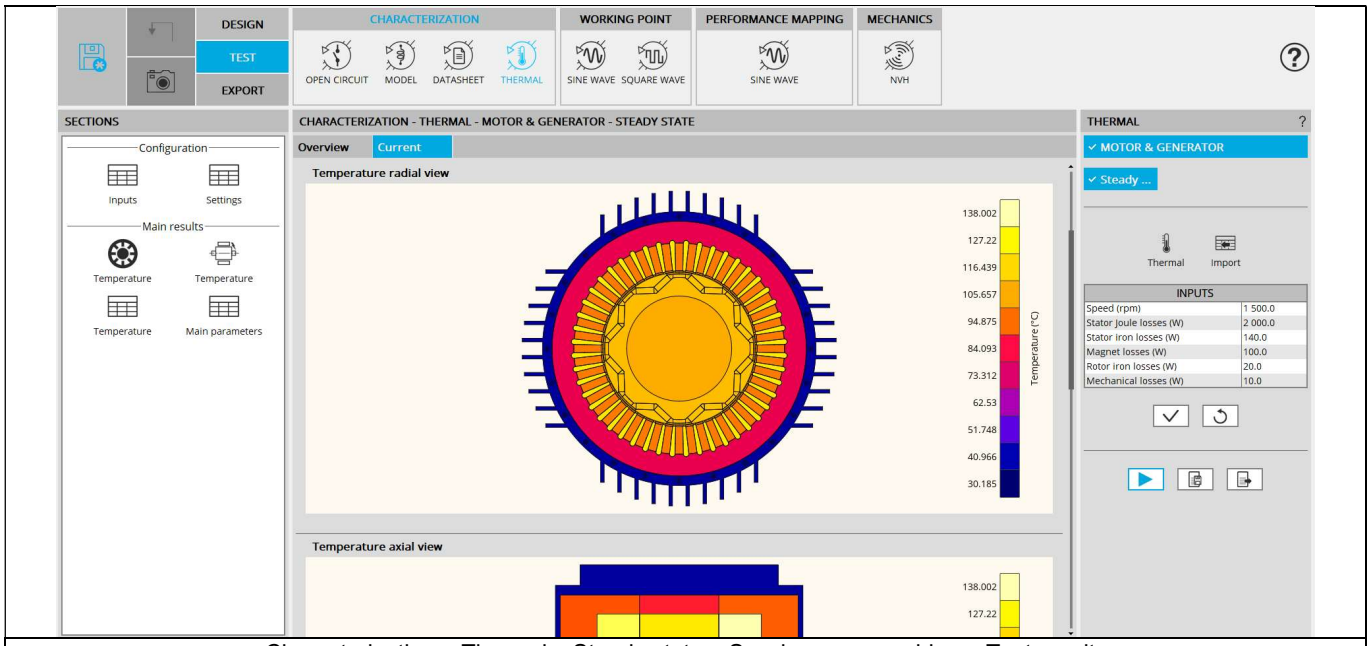

Characterization – Thermal – Steady state – Synchronous machine – Test results

5.2.2 Flow chart

Here is the flowchart illustrating the internal process of the thermal test.

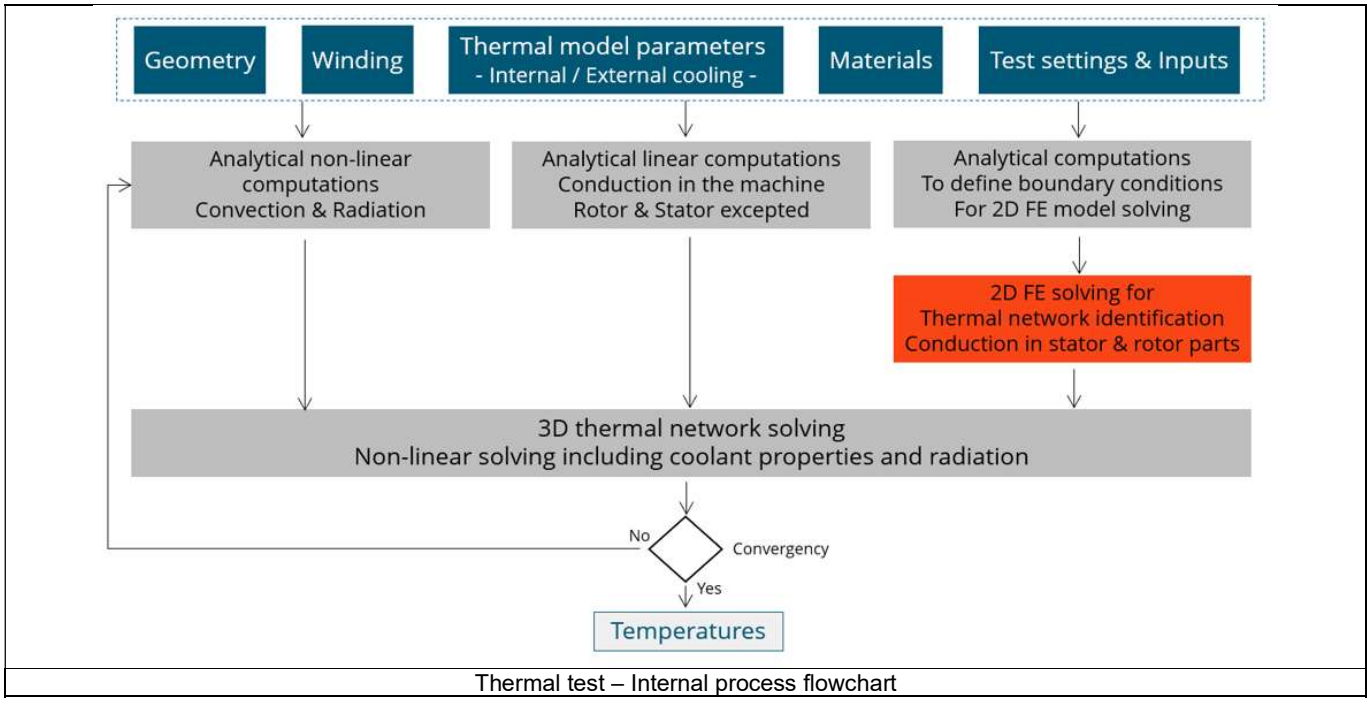

Thermal test – Internal process flowchart

The inputs of the internal process are the parameters of:

- Geometry
- Winding
- Internal cooling
- External cooling
- Materials
- Test settings and inputs

Note: A 2D Finite Element model is solved to identify a thermal network which corresponds accurately to any kind of rotor or stator parts, including user parts.

Then, the resulting network is extended with analytical computations to consider the 3D effect of the geometry.

The solving allows to get and to display the whole chart of temperatures of the machines.

5.3 Limitation of computations - Advice for use

Notes:

1) The resistance network identification of a machine is always done without any skew angle.
   This can bring some inaccuracy in the results for highly skewed machines.

2) Please refer to the document: MotorFactory_SMPM_IOR_3PH_Test_Introduction – section “Limitation of thermal computations – Advice for use”

6 CHARACTERIZATION – THERMAL – MOTOR & GENERATOR – TRANSIENT

6.1 Overview

6.1.1 Positioning and objective

The aim of “Characterization – Thermal – Motor & Generator – Transient” test is to evaluate the impact of electromagnetic performance on thermal behavior of the machine in a transient mode.
A thermal working point defined by a speed and a set of losses can be considered to compute the temperature charts and the main thermal parameters. The inputs describing the thermal working point can be set manually or imported from electromagnetic tests that were previously solved.
In addition to that, a maximum evaluation duration and a time step are added as inputs to set the transient mode.

This test helps to answer the following questions:

- Can the machine operate at the targeted working point without any overheating? Yes / No
- Can the different kinds of proposed cooling help to reach good performance? Yes / No
- How long does it take to reach the thermal steady state and what are the thermal time constants of the machine?

The following table helps to classify the test “Characterization – Thermal – Motor & Generator – Steady state”.

Family	Characterization
Package	Thermal
Convention	Motor & Generator
Test	Transient

Positioning of the test “Characterization – Thermal – Motor & Generator – Transient”

6.2 Main principles of computation

6.2.1 Introduction

Here are illustrations which give an overview of the thermal transient test:

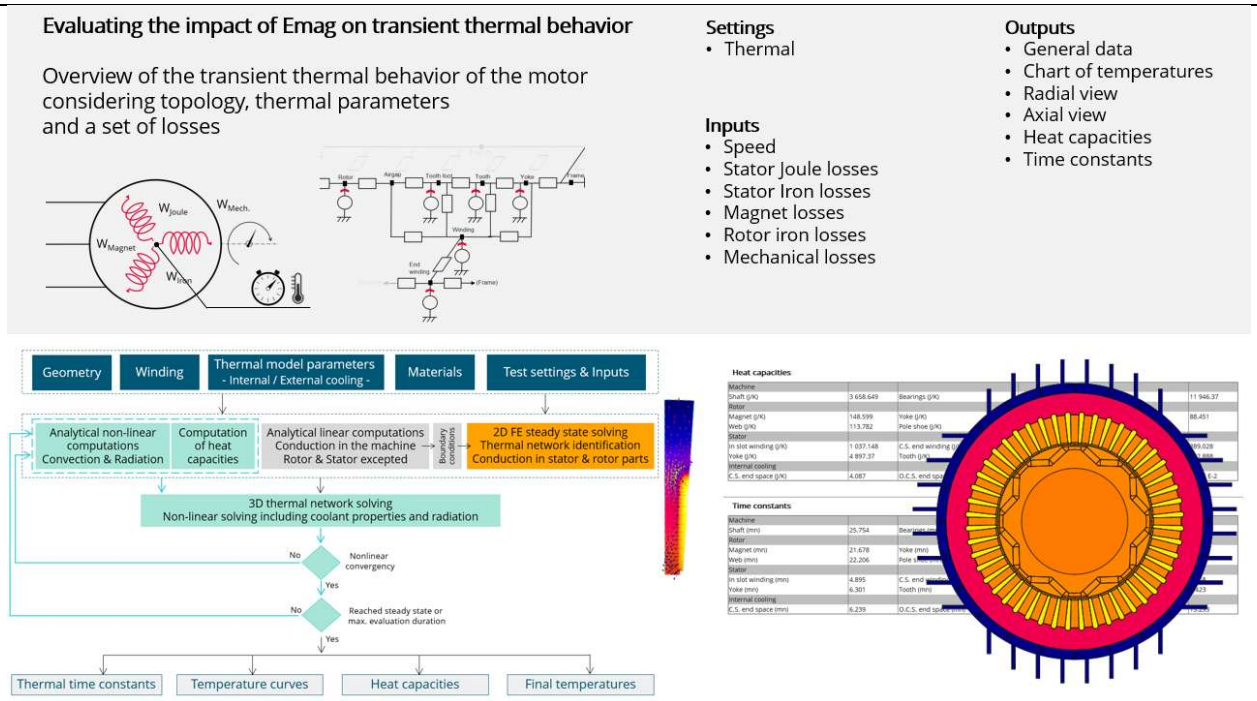

Characterization – Thermal – Transient – Synchronous machine - Overview

Characterization – Thermal – Transient– Synchronous machine – Test results

6.2.2 Flow chart

Here is the flowchart illustrating the internal process of the thermal transient test.

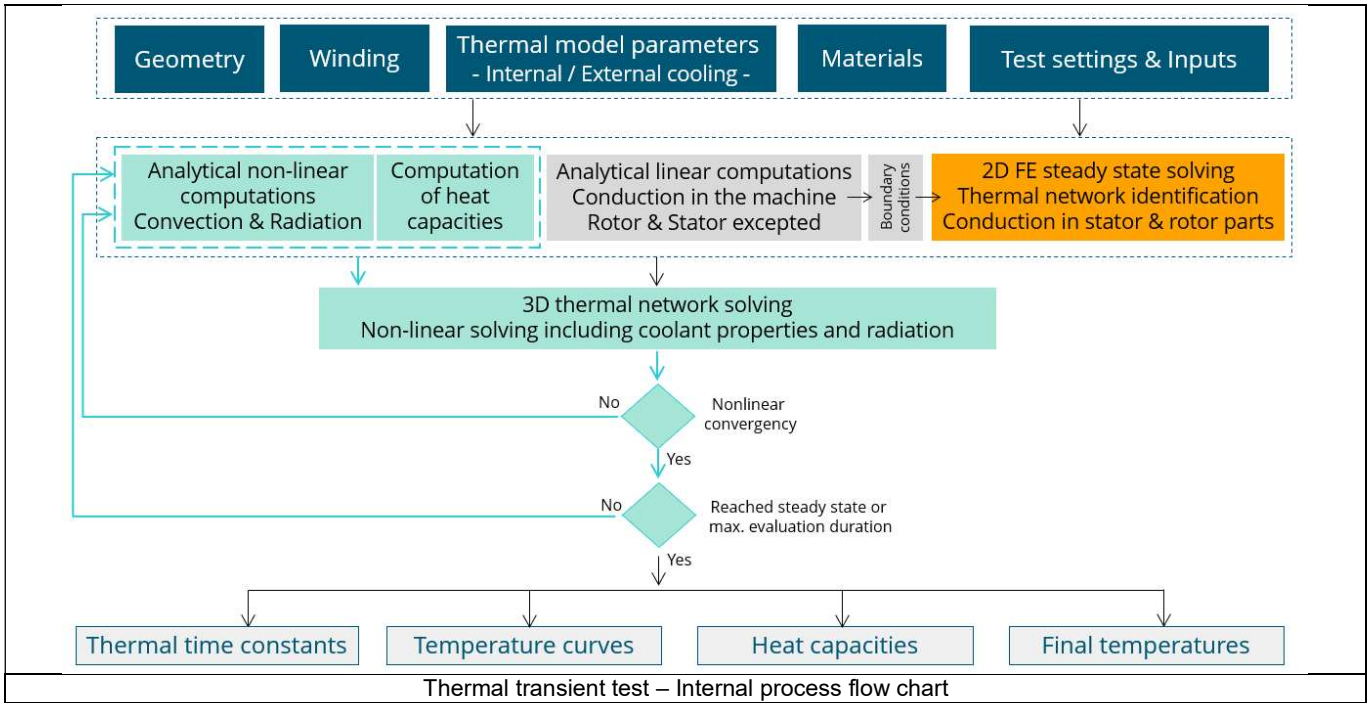

Thermal transient test – Internal process flow chart

The inputs of the internal process are the parameters of:

- Geometry
- Winding
- Internal cooling
- External cooling
- Materials
- Test settings and inputs

A 2D Finite Element model is solved to identify a thermal network which corresponds accurately to any kind of rotor or stator parts, including user parts.
Then, the resulting network is extended with analytical computations to consider the 3D effect of the geometry at each time step. For that, a non-linear computation is performed in the solving of the transient thermal test.
Each thermal node of the machine is associated to a thermal capacitance, depending of the specific heat and density of the material(s) composing the node, and the associated volume.
Thus, the main provided outputs are the whole chart of temperatures of the machines versus time, the heat capacities, and the time constants.

Note: What are the criteria that allow to see if the steady state is reached while thermal transient solving?
First, from the thermal steady state computation, one gets a good estimation of the final temperature (θ_f).
From the thermal transient computation, variation of the temperature versus the time, one deduces the inverse function, i.e. the variation of the time versus the temperature.
Knowing that the time constant to reach 63% of a temperature step is equal to:

$$\theta\tau = \theta_0 + (1- e^{-1}) \times (\theta_f - \theta_0).$$

We are looking for the time t that corresponds to $\theta\tau$. If found, it corresponds to tau.
If the evaluation time t considered is lower than τ ($t < \tau$), there is no convergency yet.
If $\tau < t < 5\tau$, there is no convergency, the thermal steady state is not reached yet, but an estimation of time needed to converge can be estimated and given to the user.
If $t > \tau$ The solving has converged, and the steady state is reached.

6.3 Limitation of computations - Advice for use

Notes:

1) The resistance network identification of a machine is always done without any skew angle.
   This can bring some inaccuracy in the results for highly skewed machines.

2) Please refer to the document: MotorFactory_SMPM_IOR_3PH_Test_Introduction – section “Limitation of thermal computations – Advice for use”

7 CHARACTERIZATION – THERMAL – MOTOR & GENERATOR – FITTING

7.1 Overview

7.1.1 Positioning and objective

The aim of the “Characterization – Thermal – Motor & Generator – Fitting” test is based on a steady state thermal computation.

Whatever the considered machine, FluxMotor creates a thermal network based on the machine topology design. However, if needed, it is possible to adjust the thermal resistances with some calibration factors (X-Factors, for external cooling as well as internal cooling) to be consistent with the measurement results for instance. This has an impact on the resulting temperatures one gets in steady state or transient mode.
The user can adjust the calibration factors, step by step, and evaluate the final temperatures by performing a manual iterative process.

This can be used either when the users want to impose the reference temperatures that are coming from measurements or when the users want to keep the same temperatures after a modification of the internal thermal architecture model.

With the test Characterization-Thermal-Motor&Generator-Fitting, the calibration for the X-factors is fully automatic. The user must target the temperatures to be obtained and the X-Factors that can be used to reach this goal. As a result, one gets X-Factors values to be applied for reaching the targeted temperatures.
This can be used either when the users want to impose the reference temperatures that are coming from measurements or when the users want to keep the same temperatures whatever the modifications of the internal thermal model architecture.

Note: This test is based on a steady state thermal computation.

Note: In the first step, this test is dedicated to the Synchronous Machines with Permanent Magnets – Inner Rotor.

The following table helps to classify the test: “Characterization – Thermal – Motor & Generator – Fitting”.

Family	Characterization
Package	Thermal
Convention	Motor & Generator
Test	Fitting

Positioning of the test “Characterization – Thermal – Motor & Generator – Fitting”

7.2 Main principles of computation

7.2.1 Introduction

Here are illustrations that give an overview of the thermal transient test:

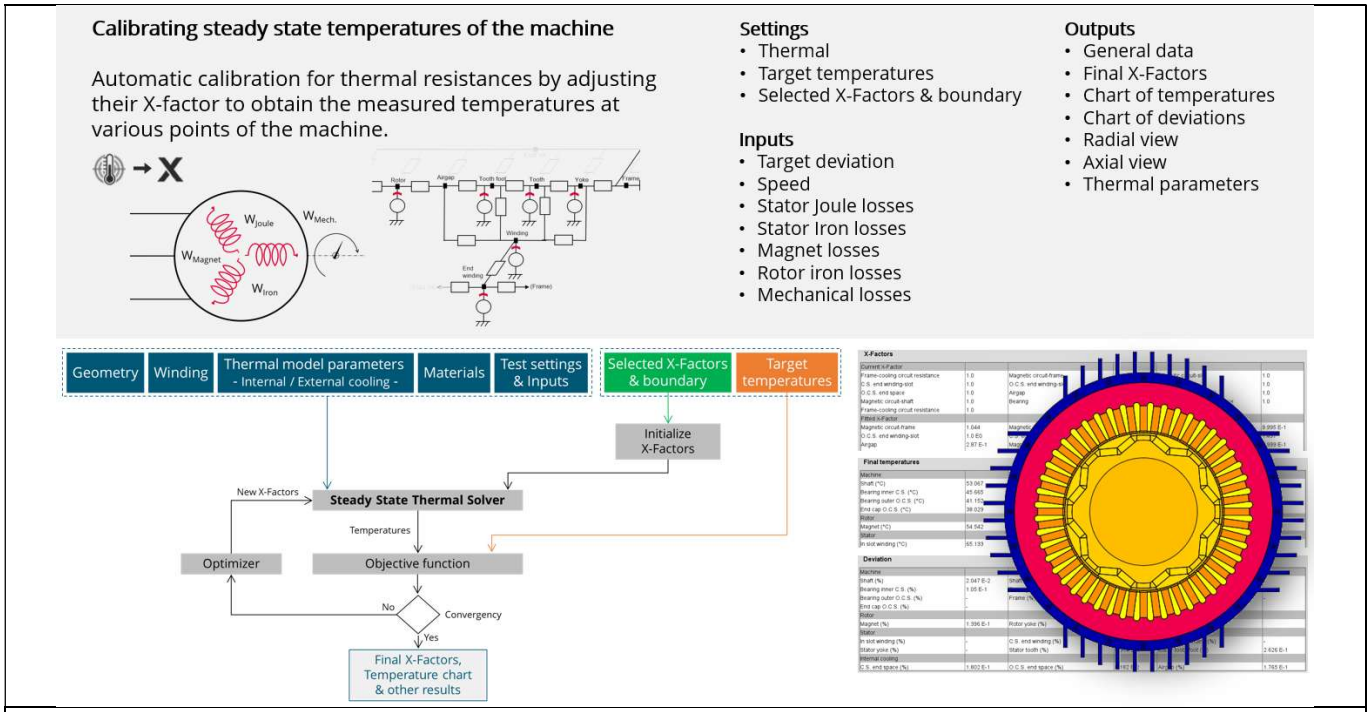

Characterization – Thermal – Fitting – Synchronous machine - Overview

7.2.2 Flow chart

Here is the flowchart illustrating the internal process of the X-Factor thermal fitting test.

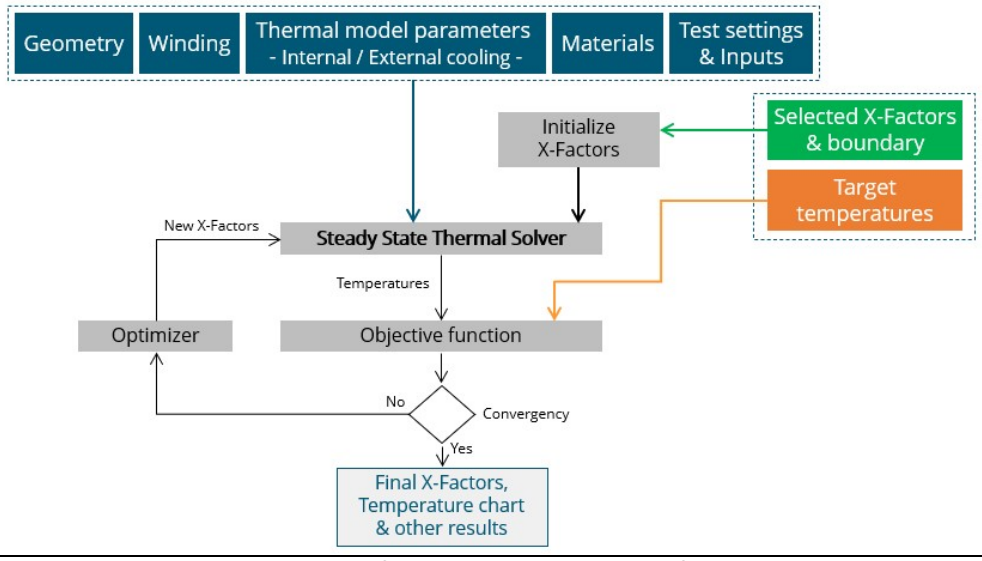

X-Factor thermal fitting test – Internal process flow chart

Note: The internal algorithm always tends to minimize the error between the target temperatures and the temperature in the model. Thanks to the "maximum resistance factor value", the variation of all the X-Factors is limited to this maximum value. Any X-Factor won't be able to exceed this maximum value. This boundary helps to stabilize the test. In case of convergency problem, it is recommended to decrease this value. The default value is set to 20.

The inputs of the internal process are the parameters of:

- Geometry
- Winding
- Internal cooling
- External cooling
- Materials
- Test settings and inputs
- + Selected X-factors and boundary for operating the fitting process.
- + target temperatures

Note: A 2D Finite Element model is solved to identify a thermal network that corresponds accurately to any kind of rotor or stator parts, including user parts.

Then, the resulting network is extended with analytical computations to consider the 3D effect of the geometry.

The solving allows to get and display the whole chart of the temperatures of the machines.

7.3 Limitation of computations - Advice for use

Notes:

1) The resistance network identification of a machine is always done without any skew angle.
   This can cause some inaccuracy in the results for highly skewed machines.

2) Please refer to the document: MotorFactory_SMPM_IOR_3PH_Test_Introduction – section “Limitation of thermal computations – Advice for use”